



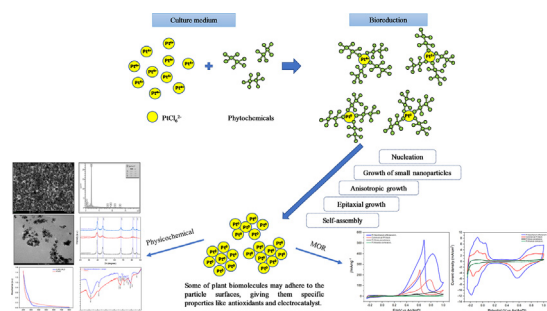
Biogenic platinum from agricultural wastes extract for improved methanol oxidation reaction in direct methanol fuel cell

N.A.I.M. Ishak^a, S.K. Kamarudin^{a,b}, S.N. Timmiati^a, N.A. Karim^a, S. Basri^a

^a Fuel Cell Institute, Universiti Kebangsaan Malaysia, 43600 UKM Bangi, Selangor, Malaysia

^b Department of Chemical and Process Engineering, Faculty of Engineering and Built Environment, Universiti Kebangsaan Malaysia, 43600 UKM Bangi, Selangor, Malaysia

GRAPHICAL ABSTRACT



ARTICLE INFO

Article history:

Received 1 May 2020

Revised 10 June 2020

Accepted 29 June 2020

Available online 02 July 2020

Keywords:

Biogenic Platinum

Direct Methanol fuel cell

Agriculture Waste

Catalyst

ABSTRACT

Platinum is the most commonly used catalyst in fuel cell application. However, platinum is very expensive, thus limits the commercialisation of fuel cell system due to the cost factor. This study introduces a biosynthesis platinum from plant extracts that can reduce the cost of platinum production compared to the conventional method and the hazardous during the production of the catalyst. The biogenic platinum was tested on a Direct Methanol Fuel Cell. Advanced biogenic of Pt nano-cluster was synthesized through a novel and facile of one-pot synthesis bio-reduction derived from natural source in the form of plant extracts as reducing agent. Several selected plant extracts drawn from agricultural waste such as banana peel, pineapple peels and sugarcane bagasse extracts were comparatively evaluated on the ability of phytochemical sources of polyphenols rich for the development of single-step synthesis for Pt NPs. Notably, the biogenic Pt NPs from sugar cane bagasse has superior electro-catalytic activity, the enhanced utilization efficiency of Pt and appreciable stability towards methanol oxidation reaction, whose ECSA value approximates $94.58 \text{ m}^2\text{g}^{-1}$, mass activity/specific activity ($398.20 \text{ mA}\text{mg}^{-1}/0.8471 \text{ mA}/\text{cm}^2_{\text{Pt}}$) which greater than commercial Pt black ($158.12 \text{ mA}\text{mg}^{-1}/1.41 \text{ mA}/\text{cm}^2_{\text{Pt}}$).

© 2020 THE AUTHORS. Published by Elsevier BV on behalf of Cairo University. This is an open access article under the CC BY-NC-ND license (<http://creativecommons.org/licenses/by-nc-nd/4.0/>).

Introduction

Fuel cells have become a promising alternative for solving energy issues where chemical energy is converted into electrical

energy without the necessity for combustion or generation of heat engine. In specifically, direct methanol fuel cells (DMFCs) have drawn significant recognition since it was developed and potentially to be used as an energy device due to several advantages, such as clean technology, generate high energy density and power, high durability, easy to operate, handle at low operating temperature and low pollutant emission [1–3]. Nevertheless, DMFCs face several circumstances that hinder their performance, such as slow

Peer review under responsibility of Cairo University.
E-mail address: ctie@ukm.edu.my (S.K. Kamarudin)

<https://doi.org/10.1016/j.jare.2020.06.025>

2090-1232/© 2020 THE AUTHORS. Published by Elsevier BV on behalf of Cairo University.

This is an open access article under the CC BY-NC-ND license (<http://creativecommons.org/licenses/by-nc-nd/4.0/>).

kinetics of methanol oxidation reaction and high cost of Pt that limits DMFCs in commercial markets [4,5].

Platinum is a favourable electrocatalyst in DMFCs because of its high durability and high efficiency toward the MOR [6,7]. In past years, many attempts have been devoted to reducing the Pt loading and its cost production while concurrently persist in to intensify the immanent activity and durability of the electrocatalyst. To this end, thriving an inexpensive catalyst design with virtues enhanced activity toward the MOR and better CO tolerance for DMFCs is an effective approach to solve this problem. Many efforts have been devoted to magnifying the effectiveness of Pt electro-catalysts, such as manipulating their morphology structures, introducing support materials and alloying Pt with other metals [8]. Of all this technique is involves conventional physical and chemical methods includes thermal evaporation, pulsed laser ablation, chemical reduction, solvothermal methods, hydrothermal methods, polyol methods, electro-spinning and electro-deposition methods [9]. However, these attempts have been fraught of laborious techniques, expensive pathway, high energy consumption, lengthy reaction times, harsh reaction, low yield and biological risks. Moreover, the noxious reducing and stabilizing agents involvement are brought concern to non-biodegradability and non-biocompatibility associated with this type of synthesis consequently, may lead to hinder large-scale applications [10]. For these reasons, developing an economically and environmentally friendly method for synthesis of platinum nanoparticle using a natural resource like plant extract aqueous through green synthesis methods is another strategy that enables to increase the efficiency of Pt electro-catalysts.

The biosynthesis of metal nanoparticles inspired from natural resources such as plant extracts happen in a single-step synthesis and one-pot reaction which offers many advantages such as that they are environmentally benign, cheap, the technique is a simple and rapid, readily scalable, they are biocompatible, thus they eliminate hazardous reagents and multistep reaction. The metabolite compounds inside plant extracts possess fantastic functional properties as surface modifiers of nanoparticles [11]. The plant extracts is comprising of primary active metabolites such as alkaloids, phenolics, proteins, terpenoids, reducing sugar, amino acids, etc., can both functionalize as reducing agents for metal ions and capping nanoparticles to prevent agglomeration [12,10]. Thus, it is possible to utilize plant extracts in manipulating the morphology and stability of nanoparticles.

Song et al. [13] first reported platinum synthesis using plant extracts, namely the *Diopyros kaki* leaf extract, and obtained a > 90% Pt NPs yield at 95 °C and with a leaf broth concentration of > 10%. Zheng et al. [14] also achieved a greater 0.5 mM Pt NPs yield at 90 °C with 70% plant extract in 25 h of reaction time, and found that the biomolecules of reducing sugar, flavonoid and protein contain in *Cacumen Platycladi* extract are good reducing agents for platinum ion reduction. Dauthal et al. [15] performed a rapid synthesis of Pt NPs employing *Punica granatum* peel extract as a template with a spherical shape and having size range of 16–23 nm. They reported that polyphenolic compounds such as ellagic acid, gallic acid, ellagic tannins and quercetin are accountable for the bio-reduction of Pt ions. Şahin et al. [16] demonstrated that Pt NPs synthesis using pomegranate extract can potentially be used for cancer treatment on human breast cancer cell line MCF-7 and showed highest inhibition of proliferation toward the cancer cell lines. It was noticed that the plant extracts carrying molecules of alcohol functional groups predominantly of the polyphenolics class and have natural antioxidant properties are potent to be exploited for redox potential along with stabilizing, growth limiting and inhibiting agglomeration, hence trigger a formation of stable complexes with Pt [17].

In this study, agriculture waste products from sugarcane bagasse (*Saccharum officinarum* L.), pineapple peel (*Ananas comosus*

L.) and banana peel (*Musa paradisiaca*) were selected to fully realize the zero-value of residue waste to high-value functionalization material in the synthesis Pt nanoparticles. The bagasse and fruit peels are polymer complexes that mainly contain cellulose, hemicellulose and lignin, which contain aromatic and phenolic groups that make them suitable as green reducing and stabilizing agents [18]. Sugarcane has flavonoids such as apigenin, luteolin and tricrin derivatives, as well as compounds of high phenolic acids such as caffeic acid, sinapic acid, and hydroxycinnamic which allow antioxidant activity [19–21]. The pineapple fruit (*Ananas comosus* L.) is a member of the *Bromeliaceae* family, contains sugar, protein-digesting enzymes, bromelain, and good amounts of citric and malic acids and vitamins, which contribute to its flavour [22,23]. Bananas (*Musa paradisiaca*) contain high fibre and are good sources of carbohydrates, minerals and vitamins [24]. Apparently, no study has tested biogenic platinum from polyphenolic group rich plant extract as electro-catalyst in methanol oxidation reaction. Therefore, the objective of this research is to comparatively evaluate the ability of agricultural wastes from aqueous extracts like pineapple peel, sugarcane bagasse and banana peel as sources of polyphenolics for the bio-reduction of single-step synthesis for Pt NPs without the need for additional capping agents or templates, hence increasing the novelty of this study. The resulting nanoparticles were extensively characterized by their physico-chemical properties using UV-VIS, XRD, TEM, FESEM-EDX, TGA-DSC and FTIR analyses. To the knowledge of the authors, there is no study that has focused on the methanol oxidation reaction using biogenic Pt NPs; therefore, the MOR is ascertained in an acidic medium and is evaluated by cyclic voltammetry analysis.

Materials and methods

All the reagents purchased were of analytical grade and were used directly. Chloroplatinic acid ($\text{H}_2\text{PtCl}_6 \cdot 6\text{H}_2\text{O}$) was procured from Merck. The agricultural wastes of sugarcane bagasse, pineapple peel and banana peel were collected from local crops. Methanol (CH_3OH , 99.2%) was purchased from Merck. Commercial Pt black HiSpec 1000 was obtained from Alfa Aesar.

Plant mediated extract preparation

The agricultural wastes of sugarcane bagasse, pineapple peel and banana peel were washed using tap water and cut into small pieces and were dried at 60 °C for several days. The dried peels were grinding in a commercial electric blender to obtain a fine powder and were stored in an airtight polymer plastic bag for further use. The fine powder was transferred into deionized water and was extraction at 60 °C for 30 min. The yellowish extracts were cooling at room temperature and filtered using muslin cloth and vacuum pump to separate any suspended substance and obtain the clear extracts. Meanwhile, fresh peel of *Musa paradisiaca* was boiled at 60 °C for 30 min without undergoing the drying process, after which it was subjected to the same process as described above. All extracts were stored in a refrigerator and were used within one week.

Green reduction of platinum nanoparticle catalyst

Pt nanoparticles were synthesized by chemical reduction using sugarcane bagasse, pineapple peel and banana peel as both reducing and stabilizer agents. The agricultural waste extracts of 10 ml were mixed with 90 ml chloroplatinic acid hexahydrate solution (1 mM) in a 1:9 ratio. The mixtures were refluxed at 95 °C and continuously stirred until colour changes from pale yellow to blackish. Then, the mixtures were sonicated for 30 min to separate the

nanoparticles from the plant extracts residue. The suspension was centrifugation at 13,400 rpm for 10 min and the recovered pellet was washed several times with deionized water and dried at 110 °C for 6 h.

Instrumentation

After the production of colloidal Pt NPs, the optical properties of the biosynthesized Pt were characterized by UV–Visible spectroscopy (Perkin Elmer, Lambda 35) in the range 200 – 800 nm. FTIR spectra of the capped functional groups of samples were measured (FTIR, Perkin Elmer, USA) in the transmittable mode over the range of 4000–400 cm^{-1} in the KBr pellets. The crystallinity and

phase structures of the powdered biosynthesized Pt NPs were investigated by XRD (D8 Advance/Bruker AXS Germany) operated at a voltage of 40 kV and current of 20 mA with $\text{Cu}/\text{K}\alpha$ radiation ($K = 1.5418 \text{ \AA}$) with scanning range (2θ) of 20 to 90°. The elemental composition was determined by EDX equipped with a Field Emission Scanning Electron Microscope (FESEM ZEISS, Model Merlin). The morphology and structure of the powdered biogenic Pt NPs were determined via Transmission Electron Microscopy (TEM, FEI Talos L120C) operating at 120 kV. Thermal analyses and decompositions of nanoparticles were performed by a TGA/DSC Mettler Toledo 851e thermal system (STARe System, Schwerzenback, Switzerland) from 25 to 1000 °C at a heating rate of 10 °C/min under an inert atmosphere with open alumina crucibles containing nanopowder samples weighing approximately 10 mg.

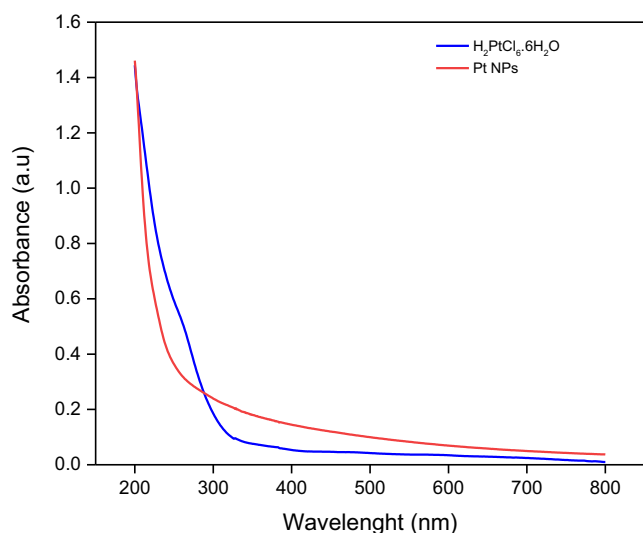


Fig. 1. UV–Visible spectra of aqueous $\text{H}_2\text{PtCl}_6 \cdot 6\text{H}_2\text{O}$ and colloidal Pt-NPs reduced by plant extracts.

Yield conversion of PtCl_6^{2-}

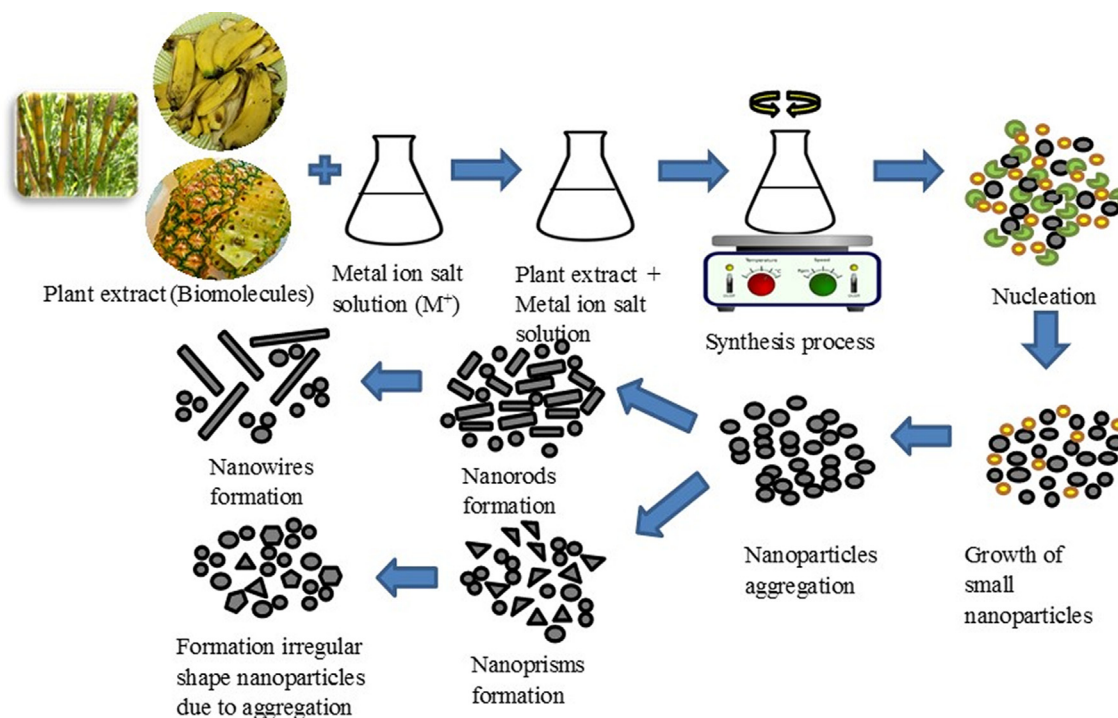
A 2.0 ml aliquot was taken from the reaction mixture and centrifuged at 13,400 rpm for 10 min. The upper layer of supernatant solution was taken out and re-centrifuged. About 10 ml of 5 wt% HCl solutions was added to the 1.5 ml aliquot of the resultant supernatant and diluted. The residual concentration of PtCl_6^{2-} was determined by an inductively coupled plasma mass spectrophotometer (ICP-MS) analyser (Thermo spectronic, USA). The conversion of Pt (IV) was calculated using the following equation:

$$x = \left(1 - \frac{m}{195C}\right) \times 100\% \quad (1)$$

where m (ppm) is the residual concentration, C (mol ml^{-1}) is the initial concentration of $[\text{PtCl}_6]^-$ and the coefficient 195 (g mol^{-1}) is the relative atomic weight of Pt.

Electrochemical measurement

The electrochemical analysis of biogenic Pt NPs was performed by cyclic voltammetry (CV) which were conducted in 0.5 M H_2SO_4 in the presence and absence of 1.0 M methanol at a scan rate of 50



Scheme 1. Mechanism proposed for NPs synthesis method using plant extracts.

mVs⁻¹ in the potential window of -0.25 to 1.0 V vs. Ag/AgCl. The electrolysis cell was powered by a potentiostat/galvanostat (Autolab PGSTAT204, Netherland) equipped with Nova 1.10 software. The instrument included a standard three-electrode system: a working electrode (glassy carbon electrode, area = 0.071 cm²), a counter electrode (Pt gauze), and a reference electrode (Ag/AgCl, sat. KCl). The glassy carbon electrode (GCE) was successively refined with 0.5 and 0.05 μm α-Al₂O₃ powder and was then sonicated in water to remove the surface adsorbed particles and to ensure a mirror-like surface. About 2 mg samples of biogenic Pt NPs were dispersed into 150 μL deionized water, 150 μL 2-propanol, and 50 μL of 5 wt% Nafion® 117 solution and ultrasonically for 5 min. 2.5 μL of the dispersions were carefully drop-coated on the GCE and left overnight at room temperature. A 10 min purge interval of N₂-saturated electrolyte liquids before running the analysis and also was used through out the experiments. A commercial Pt black was also carried out under the same conditions for comparison.

Results and discussion

UV-Visible spectroscopy of biogenic Pt NPs

Initially screening, plant extract-mediated synthesized Pt NPs were analysed using UV-Visible spectroscopy between 200 and 800 nm wavelengths. The platinum salt solution of hexachloroplatinic acid H₂PtCl₆·6H₂O has a pale yellow colour and shows characteristic UV-VIS absorption bands around 259 nm in Fig. 1. Prior to the reduction process, a threshold peak was emitted due to Pt⁴⁺ ions and were absent after reduction complete denotes to the metallic Pt⁰ nanoparticles formation. The addition sugarcane bagasse, pineapple peel and banana peel extracts to Pt ion salt causes changes in colour from transparent light yellow to a dark, blackish colour in manners of 1.5 h, 1 h and 2 h, respectively. The pH values of the plant extracts were acidic about 3 to 3.5 for all leaf extracts. The synthesis procedure of the chemical reduction that occurs between Pt ions and plant extracts is shown in Scheme 1.

FT-IR analysis of biogenic Pt NPs

The natural products that were bound specifically on the surfaces of the Pt NPs were determined using FTIR analysis to identify the possible biomolecules responsible for the bioreduction and biocapping of the reduced nanoparticles. Fig. 2 shows the absorbance bands changes associated with Pt NPs synthesized by (a) Sugarcane bagasse, (b) Pineapple and (c) Banana peel extracts before and after synthesis. According to Fig. 2 (a - c), all plant extracts have very intense and broad absorption bands at 3382.6 and 2923.6 cm⁻¹; 3340.2 and 2918.5 cm⁻¹; and 3397.4 cm⁻¹. For sugarcane bagasse, pineapple peel and banana peel, these represent O-H stretching of the alcohol or polyhydroxy polyphenolic groups and C-H asymmetrical stretching of the methylene group, indicating the possible contribution of phenolic compounds. Medium absorption peaks around 1731.3 and 1633.6 cm⁻¹; 1729.2 and 1641.4 cm⁻¹; and 1654.4 cm⁻¹ could be identified as the characteristic peaks of carbonyl group C = O stretching in carboxylic acids and free amino acids N-H of amide I and amide II stretching vibrations. The observed band at 1604.8 can be assigned to the asymmetrical stretching of -COO carboxylate of proteins and alcoholic group. A medium absorption peak at 1515.2 can be attributed to the -C = C- aromatic group. The bands observed at 1455.5 and 1373.5 cm⁻¹; and 1375.5 cm⁻¹ are associated with the C-N stretching vibration of aromatic amines [25]. The peaks at 1048.8, 1162.4, 1246.5 cm⁻¹ and 1039.0 and 1244.6 cm⁻¹ were due to C-O-C

stretching vibrations of ether and alcoholic groups [26]. A decrease in the peak intensities shown in the FT-IR spectrum of all biosynthesized Pt NPs after bioreduction process as compared to the spectrum FT-IR of sugarcane bagasse, pineapple and banana peel extract plants was clearly notified indicating the participation of the biomolecule functional groups in the Pt NPs synthesis. All of these peaks suggested the presence of polyphenolics, flavonoids and proteins in the plant extracts, which are responsible for the reduction of metal ions to metal nanoparticles.

Bioreductive mechanism of Pt NPs

Our research is focused on the power-reducing efficiency of the phytochemicals present in plant extracts, which include major polyphenolic compounds such as potential reducing agents and highly polar agents due to the abundance of polyphenolic materials in plants with high-fibre contents. The O-H and C = O groups

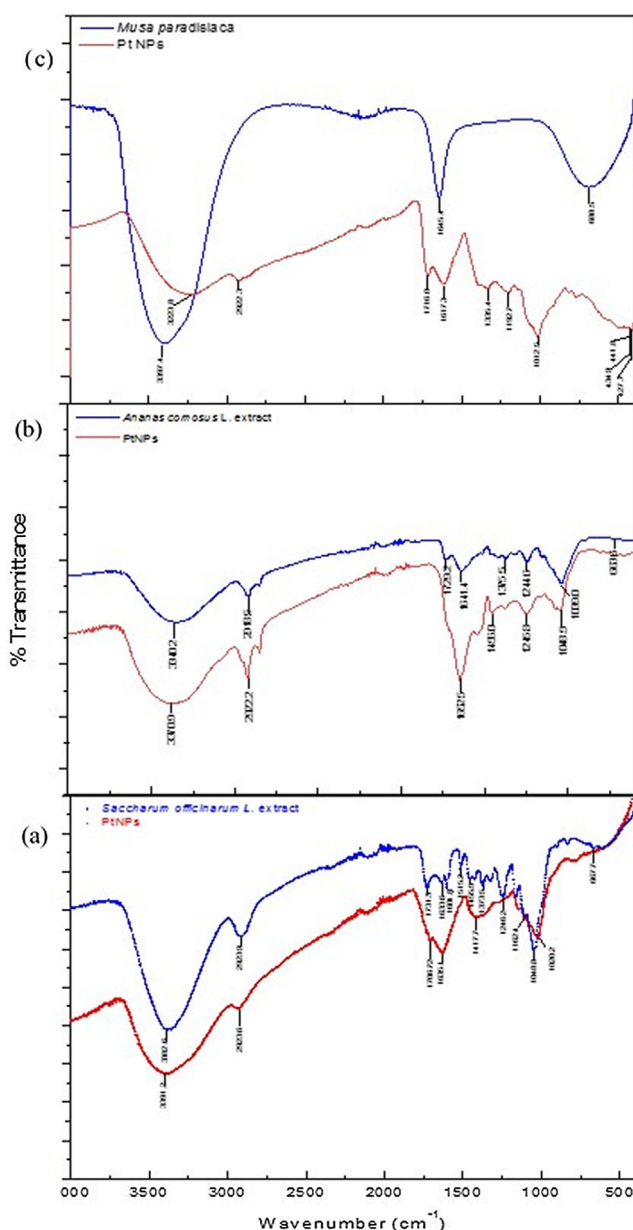
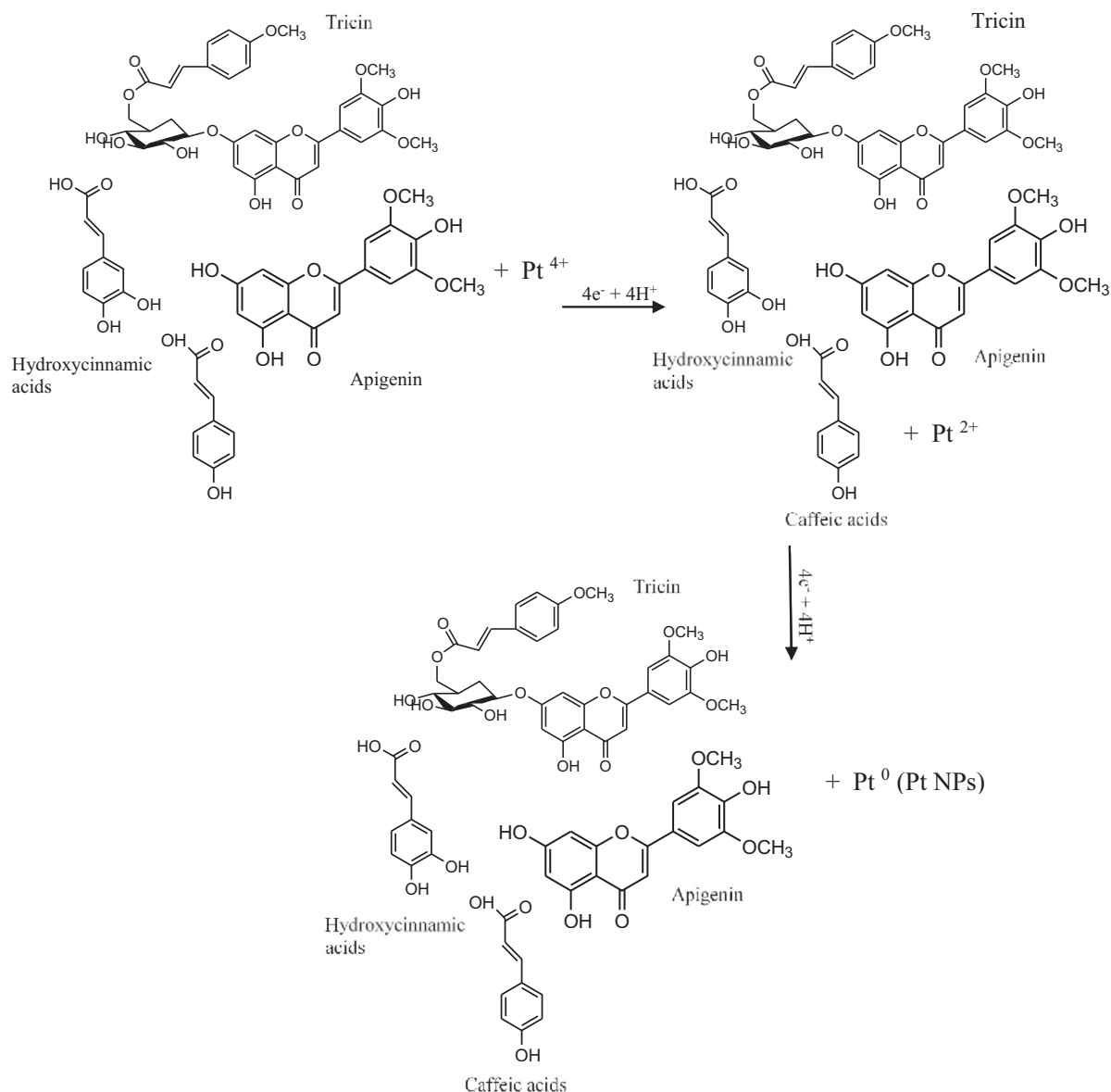


Fig. 2. FTIR spectra of (a) Pt NPs with sugarcane bagasse extract, (b) Pt NPs with pineapple peel extract (c) Pt NPs with banana peel extract.



Scheme 2. Biomolecule constituents of plant extracts involve in simultaneously chemical reduction of Pt NPs using the polyphenolic compounds such as hydroxycinnamic acids, triclin-7-O-beta-(6'-methoxycinnamic)-glucoside, caffeic acid and flavonoids like apigenin as the potent antioxidants of *Saccharum officinarum* L. bagasse extract.

Table 1

FTIR spectral analysis summary of sugarcane bagasse, pineapple and banana peel extracts and the encapsulation of biogenic Pt NPs with associated of functional groups.

Wavenumber (cm ⁻¹)	Functional group	Associated biomolecules
3382.6; 3340.2; and 3397.4	Free -OH stretching	Phenolic group, flavonoids,
2923.9; and 2918.5	C-H stretching vibration of methylene (CH ₂) group	Aromatic rings
1731.3 and 1633.6; 1729.2 and 1641.4; and 1645.4	C = O carbonyl group, N-H stretching primary amide	Carboxylic acids, free amino acids, proteins
1515.2	-C = C-	Aromatic group
1604.8	-COO carboxylate group	Proteins and alcoholic group.
1455.5 and 1373.5; and 1375.5	C-N stretching	Aromatic amines
1048.8, 1162.4 and 1246.5; and 1039.0 and 1244.6	C-O-C stretching	Ether and alcoholic groups
667.7; 663.6; and 688.5	C-H bending and CH ₂ rocking	667.7; 663.6; and 688.5

showed strong abilities to bind with metal ions due to the antioxidant properties of the plant extracts [15]. The plant extracts contain various biomolecules such as amino acids, polyphenolic acids, flavonoids and reducing sugars. These biomolecules act as reducing and capping agents of Pt NPs and can also behave like ligands, and can associate along with precursor metal ions to form complexes

[26]. Polyphenolic compounds and flavonoids are the potent antioxidants in plant extracts and are suggested to be likely involved in bioreduction mechanisms. According to the above findings, Scheme 2 shows a suggested mechanism for the bioreduction and stabilization of Pt-NPs using an exemplary polyphenolic compound of sugarcane bagasse extracts that have high-fiber contents

Table 2
Comparative analysis of synthesizing parameters to produce Pt NPs by plant extracts.

Plant origin	Conditions of synthesis		Characterisation			Application	Biomolecule	References
	Contact time	Temperature (°C)	R:M	Size (nm)	Morphology			
Piper betle L.leaf	10 min	Direct sunlight	1:9	2.1 ± 0.4 nm	Monodispersed and highly stable.	Cytotoxicity and electrochemical.	Proteins.	[1]
Cacumen Platycladi	25 h	90	N.A	2.4 ± 0.8 nm	Spherical shape. Crystalline fcc.	N/A	Reducing sugar, flavonoids and protein.	[2]
Orange peel	48 h	80	1:9	23 nm	Spherical shape. Monodispersed.	Antibacterial, Catalyst	N/A	[3]
Ocimum sanctum	1 h	100	1:9	23 nm	Irregular shape.	Water electrolysis. Electrochemical	Ascorbic acid, gallic acid, terpenoids, certain proteins and amino acids.	[4]
Mentha piperita leaf	2 h	Calcine at 450	1:4	54.3 nm	Spherical agglomerated shape. Crystalline.	Colon cancer treatment.	Polyphenols.	[5]
Gum olibanum	30 min	121	N.A	3.7–5 nm	Quasi- spherical shape. Crystalline fcc.	Colorimetric sensor.	Gum proteins.	[6]
Azadirachta indica leaf	1 h	100	1:9	5–50 nm	Spherical shape. Polydisperse.	Catalytic and thermal applications	Proteins.	[7]
Punica granatum peel	30 min	90	1:4	16 – 23 nm	Spherical shape. Crystalline fcc.	Catalyst of organic pollutant.	Polyphenolic	[8]
Taraxacum laevigatum	10 min	90	1:5	2 – 7 nm	Spherical shape. Highly dispersed.	Antibacterial.	Proteins, flavonoids and saponins	[9]
Maytenus royleanus leaf	3 h	90	N.A	5 nm	Spherical shape. Well dispersed. Crystalline fcc.	Anticancer for lung cancer cells and photo-catalyst.	Phenol, carbonyl, amide II, amine functional group	[10]
Antigonon leptopus leaf, stem and root	N.A	95	1:20	5 – 190 nm	Monodispersed spherical shape. Crystalline fcc.	N/A	Flavonoids, polysaccharides and proteins	[11]
Water hyacinth leaf	1 h	90	1:10	3.74 nm	Spherical shape.	N/A	Hydroxyl, nitrogen and carbohydrate groups	[12]
SO, MP, AN	1 – 2 h	95	1:9	2 – 17 nm	Spherical shape. Crystalline fcc. Polydispersed. Highly stable.	Electrochemical.	Flavonoids, reducing sugar and phenolic acids.	Present study

*R = Reducing agent, M = metal. **N.A. = Not available in literature. ***SO = *Saccharum officinarum* L., MP = *Musa paradisiaca*, AN = *Ananas comosus* L.

and contain hydroxycinnamic acids, triclin-7-O-beta-(6'-methoxy cinnamic)-glucoside, caffeic acid and flavonoids such as apigenin. Pt^{4+} is first chelated through a phenolic -OH group and forms an intermediate platinum complex. Because of the high oxidation-reduction (redox) potential of Pt^{4+} , the neighbouring phenolic hydroxyls were inductively oxidized to their respective quinones. During the bio-reduction reaction, the Pt^{4+} was reduced to Pt^0 in the presence of free electrons or nascent hydrogen produced. The biomolecules are also adsorbed onto the surface of Pt ions, suppressing nucleated particle growth and ultimately leading to nanoparticles formation. The adjoining Pt^0 atoms further collided with each other to form Pt-NPs. The Pt-NPs were further stabilized by quinones and polyphenolic acid compounds. Additionally, this bioreduction of Pt metal nanoparticles were compared to the previous works in Table 1 regarding in term of synthesizing parameters. Accordingly, the plant extract to metal ratio and molarity of reagents used in this study is very diluted with a shorter time and higher stability compared to previous work (Table 2).

XRD analysis of biogenic Pt NPs

Fig. 3 represent the XRD diffractogram of the crystal phase and structure of the biogenic Pt NPs. The XRD peaks of all biogenic Pt NPs synthesized by sugarcane bagasse, pineapple peel and banana peel extracts at 39.76° , 46.24° , 67.46° and 81.29° ; 39.55° , 45.99° , 67.07° and 80.75° ; and 39.27° , 45.97° , 67.31° and 80.90° were assigned to diffraction from the (111), (200), (220) and (311) Bragg's reflections of the face centre cubic (fcc) structure of metallic platinum, respectively, which agrees well with reference to the unit cell of the fcc structure (JCPDS) file no: 00-004-0802. The (111) orientation is more intense than other peaks, indicating that (111) was very high as a prevailing orientation due to a high atomic concentration and preferential adsorption of Pt atoms on that plane during the growth process, which is considered to be a highly reactive facet and the same as d-spacing. The strong and narrow peak denotes that the product has a good crystalline nature with regard to particles. There was no discernible impurity peaks were found, showing the formation of pure crystalline platinum. The Debye Scherrer's equation was used to calculate the crystallite particle sized corresponding to the XRD profile (Fig. 3) by utilizing the following formula (Eq. (2)) [27]:

$$D = K\lambda / \beta \cos\theta \quad (2)$$

where D is the average crystallite size, K is Scherer's constant ($K = 0.94$), λ is the X-ray wavelength (0.2292 nm), β is the full-width at half-maximum of diffraction line in radians and θ is the half diffraction angle. The mean sizes of Pt NPs crystallite were measured using the (111), (200), (220) and (311) planes. These calculated values of approximately 7.61 nm for sugarcane bagasse, approximately 4.86 nm for pineapple and approximately 6.05 nm for banana peel extract were congruent with the measured TEM results.

FESEM-EDX analysis of Pt NPs

Fig. 4 (a), (b) and (c) show 3D images of the morphologies features of biosynthesized Pt NPs by field emission - scanning electron microscopy (FESEM). Regarding the plant extract type, all nanoparticles synthesized were generally polydispersed and roughly spherical in shape. Accordingly, the attribution of biomolecules such as polyphenol or antioxidants in the plant extracts were success playing the key roles in as simultaneous bio-reducing and bio-stabilizer that sustain the dispersion and distribution of NPs. However, a slightly aggregated structure was observed for all samples that maybe be due to the Van der Waals' forces during the reduction process that triggered the particles to self-assembly [28]. Fur-

thermore, for the determination of the compositions of the biogenic Pt NPs, localized elemental information were ascertained from EDX. A high intense peak at 2 keV is present in the Pt region, which confirmed the formation of Pt NPs for all biogenic Pt NPs. Observable of low peaks for carbon and oxygen were appeared meaning that these elements coming from the phenolic group/active biomolecules from plant extracts bounded on the surfaces of Pt NPs. This supports the capping and stabilizing ability of organic moieties. The presence of O refers mainly to the formation of Pt oxide but may also be derived from the COO- group of phenolics compounds or other molecules containing C and O elements. High contents of Pt were reported from sugarcane (88.5%), followed by pineapple peel (81.0%) and banana peel (73.5%).

Microscopic analysis of morphology structure of biogenic Pt NPs

The TEM image further confirmed that all biogenic Pt NPs are well-dispersed and spherical shapes like presented in Fig. 5. According to Fig. 5 (a), the Pt NPs prepared using sugarcane bagasse were mainly spherical with varied in size from 2 to 17 nm with a mean size of 5 nm, which agrees well with the results obtained from FESEM images (Fig. 4 (a)). This is also close to the crystalline size of biogenic Pt NPs as estimated by Scherer's formula and as confirmed by XRD results. The HRTEM image (see Fig. 5 (c)) as recorded exhibits lattice fringes with interplanar distance of d spacing = 0.2267 nm match with the (111) reflection of crystalline fcc phase of Pt structure. As for Fig. 5 (g), the TEM image of Pt NPs synthesized by pineapple peel have size range in 8 – 25 nm with nearly spherical shape while Pt NPs synthesized by banana peel extract have spherical shape with mean size of 3 nm. HRTEM image (see Fig. 5 (f)) illustrated for Pt NPs synthesized by banana also having the d spacing of interplanar lattice fringe of 0.2261 nm which fit with the (111) reflection of fcc structure phase of Pt in XRD diffractogram. The patterns of selected region electron diffraction (SAED) for Fig. 5(b) and 5(h) display bright circular-concentric rings consequence of the random orientations of crystal planes, indicating the crystalline phase of biogenic Pt NPs. The four rings observed in SAED images represent the diffraction planes of (111), (200), (220), and (311), whereas the SAED image in Fig. 5 (e) of biogenic Pt synthesized by banana suggested that the synthesized biogenic Pt was amorphous. In

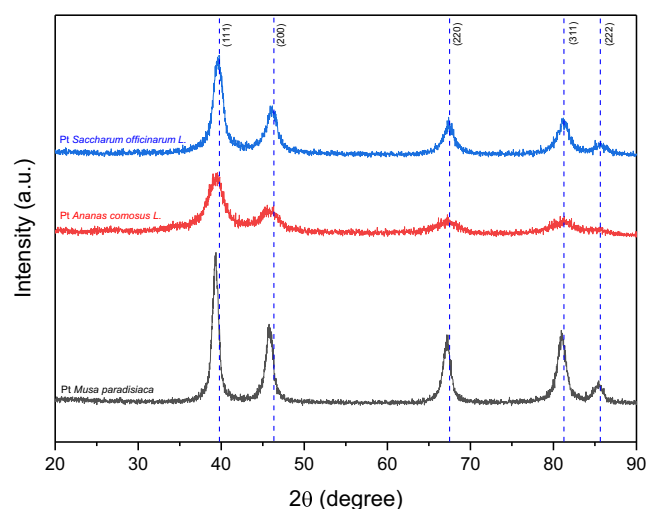


Fig. 3. XRD pattern of biogenic PtNPs using of *Saccharum officinarum* L., *Musa paradisiaca*, *Ananas comosus* L. and extract comply with reference standard of JCPDS file No. 04-0802 of pure Pt.

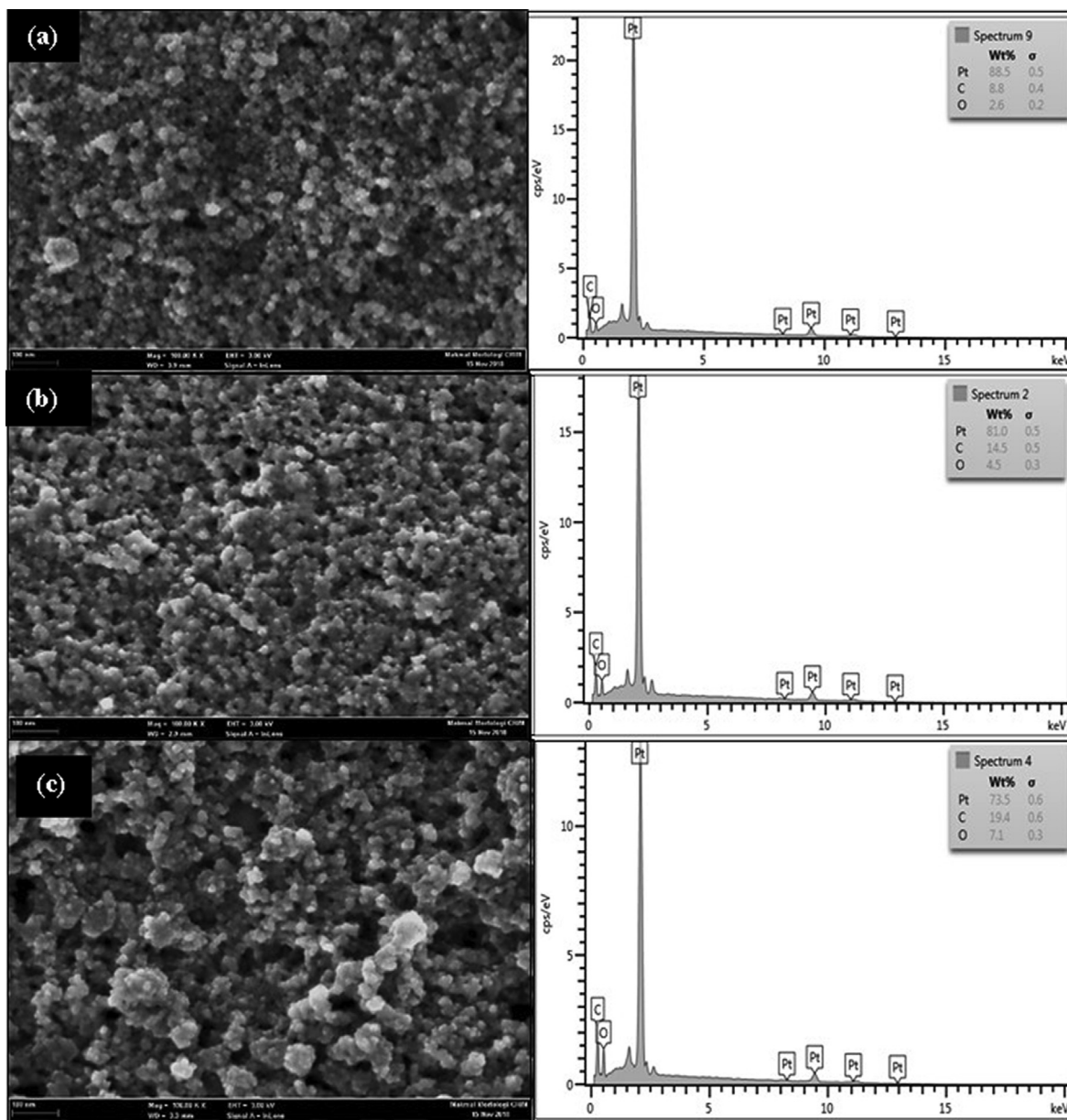


Fig. 4. (a, b, c) FESEM images with EDX spectrum quantitative analysis synthesized PtNPs using (a) *Saccharum officinarum* L., (b) *Ananas comosus* L. and (c) *Musa paradisiaca* aqueous broth extract.

addition, it is notable that a thin layer of biomatrix was observed in all TEM images, suggesting that the Pt NPs resided in the nanoscopic template of biomolecules present in plant extracts.

Thermal properties

Residual plant extracts bonded on the surfaces of the Pt NPs were assessed using TGA/DSC. Thermal degradation of the biogenic Pt NPs using plant extracts included heating from 25 to 1000 °C under an inert nitrogen atmosphere, with results shown in Fig. 6. All TGA/DSC thermograms show similar thermal decomposition trends with two stages. The first decomposition stage occurs is the desorption of water while the second stage involves the thermal degradation biomolecule compounds bounded on the surface of biogenic Pt NPs [25]. A small total weight loss of –8.64% occurs for the Pt NPs synthesized by of sugarcane bagasse while total weight losses of –14.75 and –22.85% occur for the Pt NPs synthesized by pineapple peel and banana peel, respectively. These stip-

ulate the existence of small amounts of impurities and organic residue in the Pt NPs synthesized by the plant extracts. The initial weight loss that occurs during the first decomposition step of all biogenic Pt NPs up to 156 °C is the removal of strongly coordinated water molecules via the condensation of hydroxyl with external water molecules. The transition is supported by the appearance of an endothermic DSC peak at approximately 140 °C. Then, the Pt NPs show steady weight loss beginning at 150 °C, with thermal decomposition ending at 800 °C, which due to the decomposition of organic compounds that is most likely resulting from the surface desorption of the organic compounds present in the nanoparticle powder. Slight, further degradation was observed in thermogram of the Pt NPs synthesized by banana peel extract, but no further degradation was observed after 800 °C for the Pt NPs synthesized by sugarcane bagasse and pineapple extracts resulted in a nearly horizontal curve, which suggests the stability of elemental platinum. The thermo-gram of all biogenic Pt NPs exhibited excellent thermal stability.

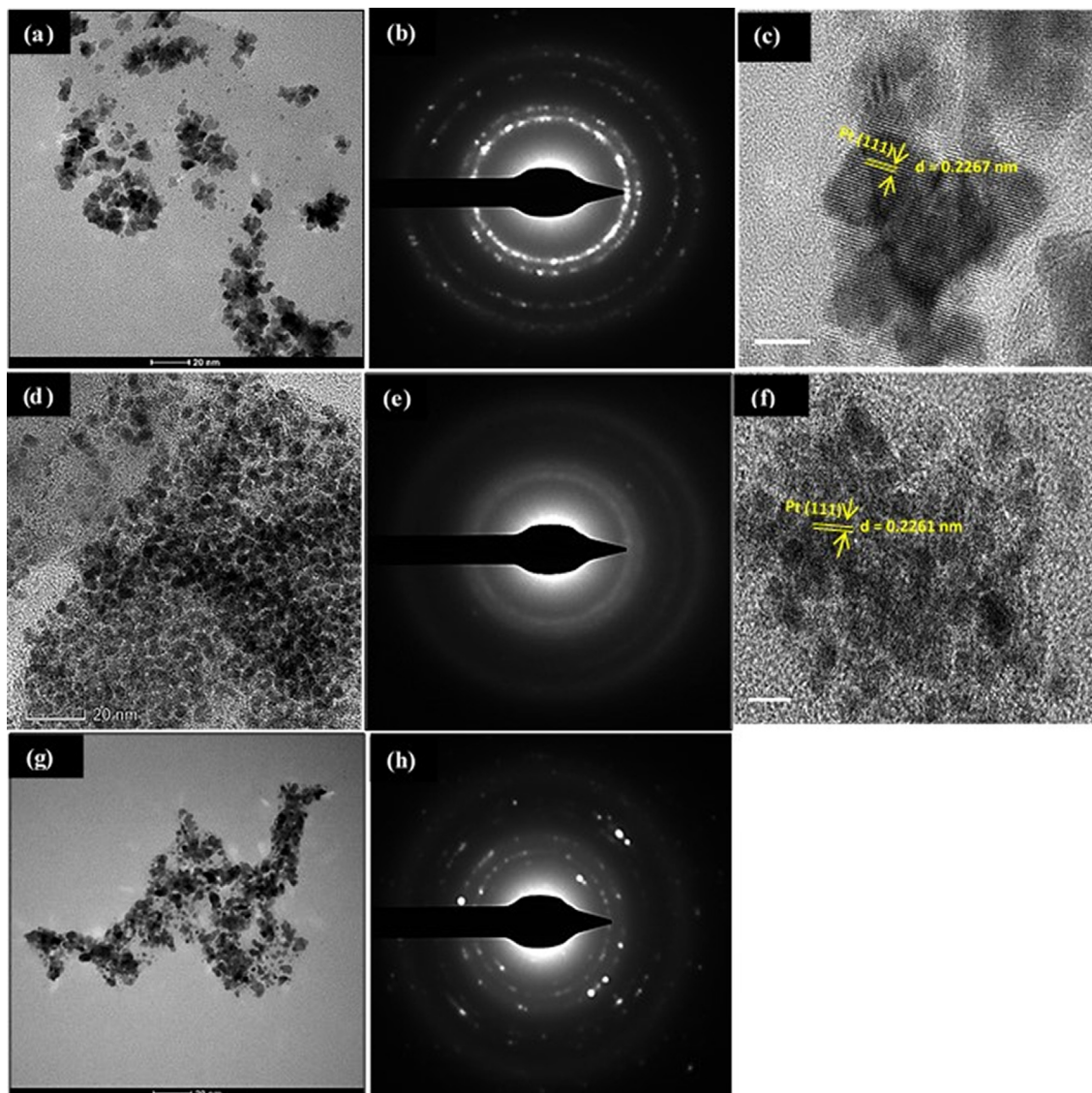


Fig. 5. Show TEM image of synthesized PtNPs by plant extracts of (a) *Saccharum officinarum* L., (b) *Ananas comosus* L. and (c) *Musa paradisiaca* aqueous broth extract.

Assessment of electrochemical properties of synthesized biogenic Pt NPs

H_2 adsorption and desorption

The electro-catalytic activity of all biogenic Pt NPs was studied in an acidic medium by voltammetric measurements at room temperature with a saturated N_2 purge during the experiments. Fig. 7 (a) and (b) show the cyclic voltammograms (CVs) normalized to catalyst loading and the geometric area of the working electrode. The typical CV curve used to determine the hydrogen and oxygen absorption on all catalysts were evaluated in 0.5 M H_2SO_4 at scan rate of 50 mV s^{-1} in the potential window of -0.25 to 1.0 V vs Ag/AgCl at room temperature to quantify the ECSA values of different catalysts. The ECSA values of the respective catalysts calculated from the integrated charge area under the hydrogen adsorption peak, which represents the total charge (Q_H) after deducting the area that corresponds to double-layer charging in the CV, using below equation [29]:

$$ECSA(m^2.g^{-1}) = \frac{Q_H(Cm^{-2})}{2.1(Cm^{-2})\chi[Pt](gm^{-2})} \quad (3)$$

where Q_H is the charge for hydrogen adsorption ($C m^{-2}$), $[Pt]$ represents the platinum loading ($g m^{-2}$) on the working electrode and $2.1 (C m^{-2})$ is the charge required to oxidize a monolayer of H_2 onto the Pt surface.

From Fig. 7 (a), the voltammogram reveals information associated hydrogen adsorption/desorption area and the oxide formation/reduction area on the Pt NPs surfaces. As observed, the CVs show strong characteristics of hydrogen absorption/desorption peaks below approximately 0.2 V and Pt oxidation/reduction peaks beyond approximately 0.4 V . The higher potential peak at approximately 0.56 V is associated to the Pt-oxide reduction ($Pt + H_2O \rightarrow Pt-OH + H^+ + e^-$ [30]) on the biogenic Pt NPs surface during a forward scan (anodic sweep) [31]. The characteristic peak at lower potential in the -0.25 to 0.1 V region is the monolayer hydrogen adsorption/desorption on the Pt-NPs active surface. The calculated ECSA value for Pt NPs-sugarcane bagasse was 94.58 m^2g^{-1} , which is much higher than those of Pt NPs-banana peel extract (3.69 m^2g^{-1}), Pt NPs-pineapple peel extract (1.69 m^2g^{-1}) and commercial Pt black (27.49 m^2g^{-1}). However, the hydrogen adsorption and desorption regions in the CV of Pt NPs-banana and Pt NPs-pineapple were very small, suggesting that the organic

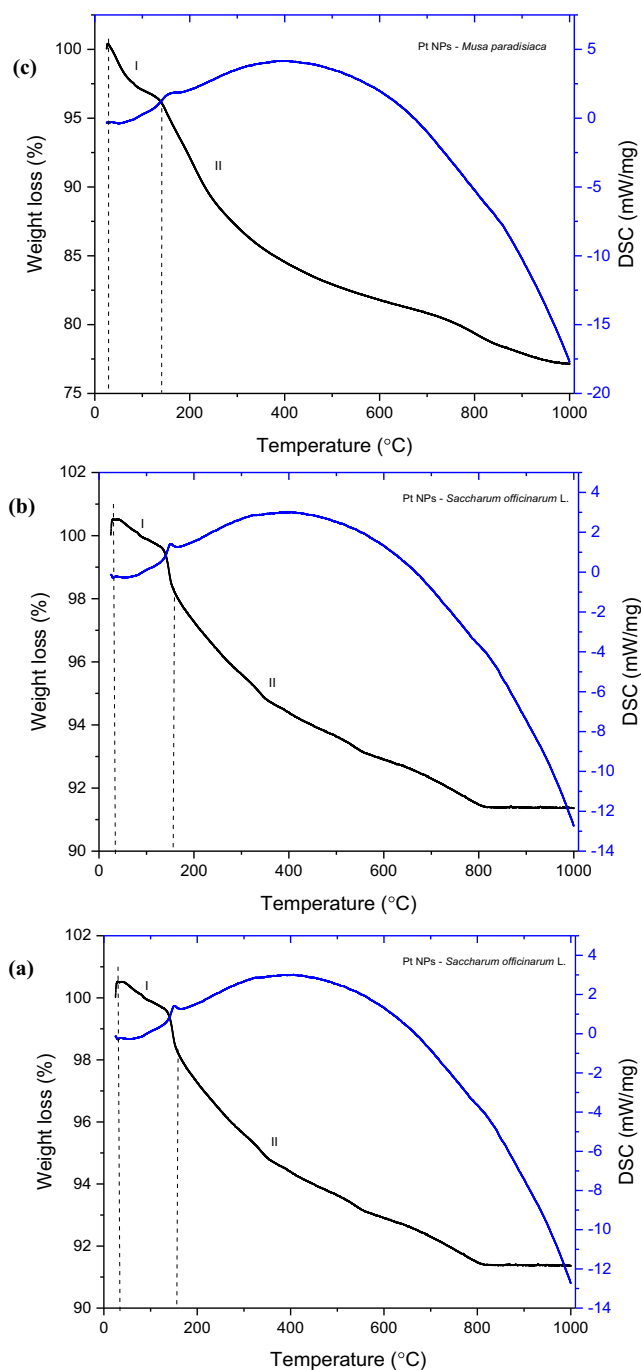


Fig. 6. TGA/DSC thermogram of synthesized biogenic Pt NPs of (a) *Saccharum officinarum* L., (b) *Ananas comosus* L. and (c) *Musa paradisiaca* aqueous broth extract.

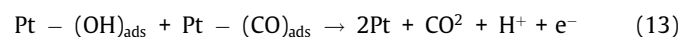
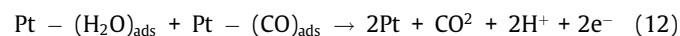
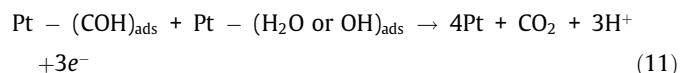
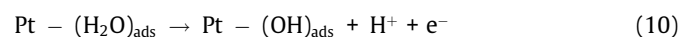
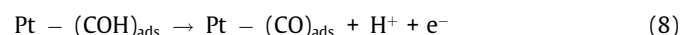
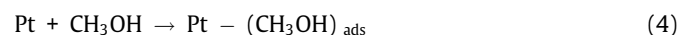
molecules may block the active sites of the Pt particles. In addition, other contributing factor is may be due to the limited interaction during bio-reduction between platinum precursors with plant extract of pineapple peel extract and banana peel extract and lack of sufficient functional groups that lead to un-complete reduction. This order is similar to findings reported by Prabhuram et al. [32] and Guo et al. [33], who noted no characteristic features associated with hydrogen absorption/desorption due to the complete blocking of Pt active sites by surfactant molecules.

The biogenic Pt NPs-sugarcane exhibited a dramatically superior ECSA, approximately 3.44 times that of commercial Pt black, demonstrating a significantly improved electrochemical activity

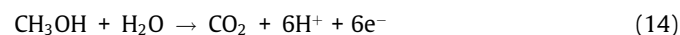
on Pt NPs synthesized by plant extracts. It seems that more active sites are available for H_2 adsorption/desorption and help improve the electro-oxidation of the methanol reaction. The higher ECSA value is attributed to the presence of well-dispersed and very fine Pt particles, as illustrated in the TEM image resulting from functionalized active biomolecules from plant extracts. The particle sizes also play in the catalyst's catalytic activity as most of the chemical reactions occur on the catalyst's surface; therefore, decreasing particle size leads to an increase in catalytic activity [34]. The uniform size and good dispersion of Pt nanoparticles is thought to produce a larger accessible surface area of active site, thus promoting a higher catalytic activity than aggregated nanoparticles. Furthermore, the onset potential (E_{onset}) Pt NPs of all plant extracts are shifted to negative potential in accordance of $0.203\text{ V} \leq 0.205\text{ V} < 0.278$: Pt NPs-banana peel extract \leq Pt NPs-pineapple peel extracts $<$ Pt NPs-sugarcane compared to Pt black commercial of 0.313 V.

Methanol oxidation reaction

The electrocatalytic performance toward the methanol electro-oxidation for all biogenic Pt NPs (Pt NPs- sugarcane, Pt NPs- banana peel extract, Pt NPs- *A. comosus* pineapple peel extracts) and commercial Pt black were evaluated by the CVs in 0.5 M H_2SO_4 + 1.0 M CH_3OH . Fig. 7 (b) clearly shows the CV curves of forward anodic peaks and reverse cathodic peaks for different biogenic electrocatalysts for methanol oxidation. The oxidation peak in the forward scan at the range of about $-0.65 - 0.84\text{ V}$ is the characteristic peak for methanol oxidation on the Pt surfaces with the formation of carbonaceous intermediate such as CH_2OH_{ads} , $CHOH_{ads}$, CHO_{ads} and the strongest adsorbed CO species, and species will oxidized to Pt-OH and Pt-O species at higher potential [35]. Whereas the reverse scan peak emerged at a range of about $-0.4 - 0.67\text{ V}$ corresponds to the efficiency of the removal of carbonaceous species that were generated during the forward scan of methanol oxidation. Generally, as described by others, possible oxidation reactions of the methanol are as follow [4]:



The total electro-oxidation of methanol is expressed as:



As shown in Fig. 7 (b), biogenic Pt NPs- sugarcane had the highest mass activity of 398.20 mA/mg_{Pt} compared to the other two biogenic Pt NPs and was 2.52 times greater than that of commercial Pt black (158.12 mA/mg_{Pt}). The onset potential (E_{onset}) of

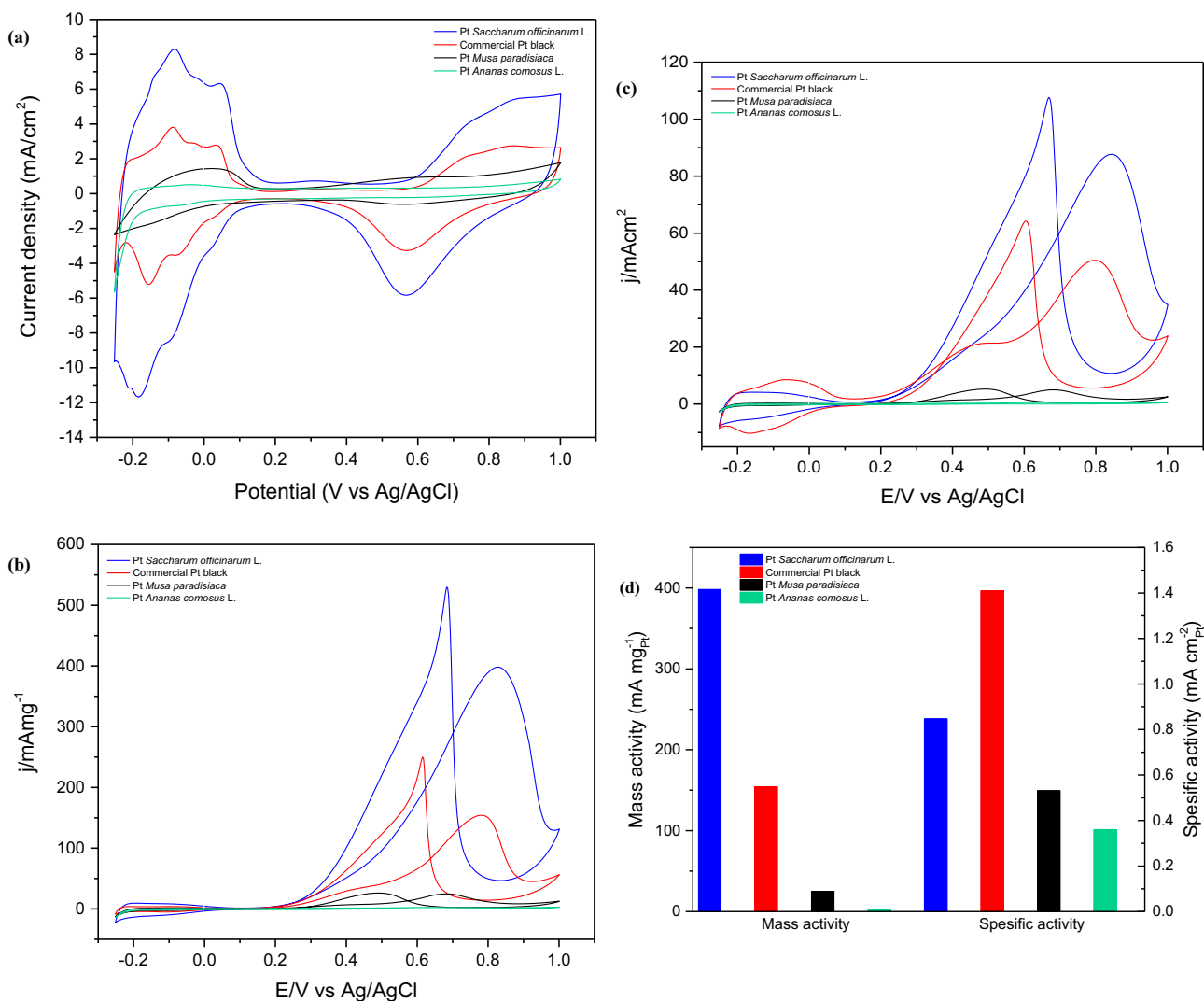


Fig. 7. (a) Represent the H₂ absorption and desorption of Pt catalyst in 0.5 M H₂SO₄ electrolyte at 50 mV/s; (b, c) CV curves in 0.5 M H₂SO₄ and 1.0 M CH₃OH aqueous at 50 mV/s and (d) histogram of mass activity and specific activity for biogenic electrocatalyst Pt NPs.

Table 3
Comparison of the electrochemical activities of biosynthesized Pt NPs and commercial Pt black towards MOR.

Catalyst	ECSA (m ² /g of Pt)	Peak potential (V vs Ag/AgCl)	Onset potential (V vs Ag/AgCl)	Mass activity (mA/mg _{Pt})	Specific activity (mA/cm _{Pt} ²)	Peak current density (mA/cm ²)	CO tolerance I _f /I _b ratio
Pt <i>Saccharum officinarum</i> L.	94.58	0.844	0.278	398.20	0.847	87.68	0.81
Commercial Pt black	27.49	0.801	0.313	158.12	1.410	50.48	0.79
Pt <i>Musa paradisiaca</i>	9.91	0.681	0.203	37.56	2.048	4.985	0.94
Pt <i>Ananas comosus</i> L.	1.69	0.644	0.205	2.52	0.360	0.609	0.83

methanol oxidation given by all biogenic Pt NPs show shifts to more negative values with following order: Pt NPs-banana peel extract (0.203 V) ≤ Pt NPs-pineapple peel extract (0.205 V) < Pt NPs- sugarcane bagasse (0.278 V) than commercial Pt black (0.313 V), which means that faster of methanol oxidation reaction can happen where it only require lower potential to perform. The Pt NPs-sugarcane bagasse displayed the highest current density at approximately ~0.84 V vs Ag/AgCl in an anodic sweep and at approximately ~0.67 V vs Ag/AgCl in a cathodic sweep. These results are reflected to the electrocatalytic activity of the catalyst

which strongly demonstrated the enhancement of catalytic activity of the Pt NPs in MOR synthesized using green chemical reduction from plant extracts.

According to histogram in Fig. 7 (d), further analysis on efficiency utilization of Pt mass can be investigate from the specific activity (mA/cm_{Pt}²) where Pt NPs-sugarcane bagasse displayed remarkable high mass activity approximately 398.20 mA/mg with small amount utilization of specific activity (mA/cm_{Pt}²) approximate 0.84711 mA/cm_{Pt}² as compared to others Pt electro-catalyst where using high utilization of Pt mass accordingly to the specific activity

Table 4
Comparison of methanol electro-oxidation on various method.

Catalyst	Type of catalyst and morphology	Synthesis methods	ECSA (m^2/g of Pt)	Peak potential (V vs Ag/AgCl)	Peak current density (mA/cm^2)
This study	Pt cluster	Biosynthesis using plant extract <i>Saccharum officinarum</i> , L.	94.58 m^2g^{-1}	0.84	87.68 mA/cm^2 , 398.20 mA/mg
Kong et al. [36]	Pt sponge-like	Photochemical synthesis	31.73 m^2g^{-1}	0.73	340 mA/mg
Shi et al. [38]	PtPd sheet-assembled network	Conventional wet-chemical reduction	38.65 m^2g^{-1}	0.95	26.6
Ojani et al. [4]	Pt needle-flower like	Electrodeposition	0.42 cm^2	0.64	87.7 mA/mg
He et al. [30]	PtAu stellated morphology	Conventional wet-chemical reduction	64.2 m^2g^{-1}	–	48.03
Han et al. [41]	CuPt stellated morphology	Seed-mediated	42.1 m^2g^{-1}	0.61	0.73
Wang et al. [37]	Pt nanosponge foil	Conventional wet-chemical reduction	25.98 m^2g^{-1}	0.85	192.02 mA/mg
Yang et al. [39]	PtPd porous nanostructure	Polyol reduction	31.59 m^2g^{-1}	–	210.35 mA/mg
Yang et al. [40]	PtPd hollow	Galvanic replacement reaction	19.7 cm^2	~ 0.7	346.8 mA/mg
Li et al., [35]	PtAg octahedral	Hydrothermal	57.48 m^2g^{-1}	~ 0.67	372.3 mA/mg

histogram. This implying that Pt NPs-sugarcane bagasse succeeded possess of extraordinary catalytic activity. The forward anodic peak current density of Pt NPs-sugarcane bagasse (87.68 mA cm^{-2}) exhibited the highest peak of current density where can be explained a higher number of electrons was generated, showing an enhanced electrocatalytic activity of the methanol oxidation reaction. The enhanced electrochemical activity of Pt NPs-sugarcane bagasse can be explained due to the well-dispersed and uniform size of Pt particles and higher value of ECSA leading to large electrochemical number of active sites. Additionally, the ratio of the forward peak current density (I_f) to the backward peak current density (I_b) was conceived to characterize the tolerance on the electrocatalyst surface to the accumulation of carbon-containing intermediate species. The I_f/I_b ratio voltammetry profiles shows that the sequence of is Pt NPs-banana peel extract (0.94) > Pt NPs-pineapple peel (0.83) > Pt NPs-sugarcane (0.81) > commercial Pt black (0.79). The I_f/I_b value indicates to the response of the methanol oxidation to CO_2 and the accumulation of carbon-derived species, though known that Pt catalyst is easily poisoned by the CO intermediate species, hence the results displayed by all biogenic Pt NPs is appreciable. The functionalized active biomolecules involved via the bio-reduction synthesis method succeed to dramatically increase the methanol oxidation reaction however, the CO tolerance is needed further adjustment. Table 3 summarizes the overall performance of the synthesized catalysts based on the CV analysis and evaluation between the regions of methanol oxidation potential in acidic media.

Evaluation of methanol electro-oxidation on various electrodes

The comparison of Pt NPs- sugarcane bagasse with other Pt-based catalysts in terms of synthesis method and electrocatalytic performance in MOR reported in recent years were summarized in Table 4. Interestingly to note that the electrochemical performance of the biosynthesized Pt NPs is superior than Pt-based materials synthesized by conventional methods, such as wet-chemical reduction with vary morphologies of Pt sponge-like structure [36], Pt nanosponge foil [37], bimetallic PtPd sheet-assembled network [38], bimetallic PtAu stellated morphology [30], bimetallic PtPd porous nanostructure [39] and other conventional technique such as electrodeposition of Pt needle-flower like structures [4], galvanic replacement reaction of PtPd hollow [40], hydrothermal technique of PtAg octahedral shape [35] and seed-mediated approaches of bimetallic CuPt stellated morphologies [41]. Clearly, the power density for Pt NPs-sugarcane bagasse showed the highest performance compared to other catalysts. The resulting synthesized Pt NPs- sugarcane bagasse in the direct methanol fuel cell (DMFC) performance as anode material has displayed extraordinary activity than the commercial Pt black catalyst. Thus, CH_3OH molecules in contact with Pt NPs synthesized

using sugarcane bagasse extract, affirming that Pt NPs functionalized by active biomolecules as electrocatalyst plays a significant value in the electrocatalytic performance where demonstrated superior efficient electron transfer during the MOR.

Conclusion

The present study is the first of its kind that presents the preparation, characterization and chemical activities of biogenic Pt NPs and their catalytic properties toward the methanol oxidation reaction for fuel cell applications. This paper presents a novel, one-pot facile synthesis and environmentally benign to prepare a novel biogenic Pt nano-clusters electro-catalyst through bio-reduction functionalised by active biomolecules present in plant extracts and comparing the results to other studies of reducing agents in chemical bio-reduction methods. Pt NPs-sugarcane bagasse extract exhibited the most enhanced ECSA, mass activity and efficient Pt mass utilization for the MOR relative to other Pt NPs plant-mediated synthesis (Pt NPs-*M. paradisiaca* and Pt NPs-*A. comosus* L.) and to commercial Pt black. It presented the highest ECSA as 94.58 m^2/g and greater specific (mass) activity as 398.20 mA/mg . This may be attributed to the highly dispersed and uniform size of Pt NPs effects from the stabilizing and functionalized effect of functional organic molecules inside the plant extract of sugarcane bagasse and more active reaction sites in the morphology/structure were exposed, in which the smallest particle sizes will provide a larger surface area, leading to kinetic activity in methanol oxidation reaction. This facile one-pot synthesis obviously offers a new strategy for high-performance DMFCs and reduces the strategy cost of production.

Declaration of Competing Interest

The authors declared that there is no conflict of interest.

Acknowledgement

We gratefully thank you to the Ministry Of Higher Education (MOHE) MALAYSIA under grant: TRGS/1/2018/UKM/01/6/2 and Universiti Kebangsaan Malaysia under grant: DIP-2019-021

Appendix A. Supplementary material

Supplementary data to this article can be found online at <https://doi.org/10.1016/j.jare.2020.06.025>.

References

- [1] Chang R, Zheng L, Wang C, Yang D, Zhang G, Sun S. Synthesis of hierarchical platinum-palladium-copper nanodendrites for efficient methanol oxidation. *Appl Catal B Environ* 2017;211:205–11. doi: <https://doi.org/10.1016/j.apcatb.2017.04.040>.
- [2] Kamaruddin MZF, Kamarudin SK, Daud WRW, Masdar MS. An overview of fuel management in direct methanol fuel cells. *Renew Sustain Energy Rev* 2013;24:557–65. doi: <https://doi.org/10.1016/j.rser.2013.03.013>.
- [3] Ahmad MM, Kamarudin SK, Daud WRW, Yaakub Z. High power passive μ DMFC with low catalyst loading for small power generation. *Energy Convers Manag* 2010;51:821–5. doi: <https://doi.org/10.1016/j.enconman.2009.11.017>.
- [4] Ojani R, Hasheminejad E, Raoof JB. Direct growth of 3D flower-like Pt nanostructures by a template-free electrochemical route as an efficient electrocatalyst for methanol oxidation reaction. *Energy* 2015;90:1122–31. doi: <https://doi.org/10.1016/j.energy.2015.06.061>.
- [5] Sadhukhan M, Kundu MK, Bhowmik T. Highly dispersed platinum nanoparticles on graphitic carbon nitride : A highly active and durable electrocatalyst for oxidation of methanol, formic acid and formaldehyde. *Int J Hydrogen Energy* 2017;42:2097–10. doi: <https://doi.org/10.1016/j.ijhydene.2017.03.097>.
- [6] Tao W, Pan D, Gong Z, Peng X. Nanoporous platinum electrode grown on anodic aluminum oxide membrane: Fabrication, characterization, electrocatalytic activity toward reactive oxygen and nitrogen species. *Anal Chim Acta* 2018;1035:44–50. doi: <https://doi.org/10.1016/j.aca.2018.06.076>.
- [7] Escobar Morales B, Gamboa SA, Pal U, Guardiola R, Acosta D, Magaña C, et al. Synthesis and characterization of colloidal platinum nanoparticles for electrochemical applications. *Int J Hydrogen Energy* 2010;35:4215–21. doi: <https://doi.org/10.1016/j.ijhydene.2010.01.040>.
- [8] Abdullah N, Kamarudin SK. Novel Anodic Catalyst Support for Direct Methanol Fuel Cell: Characterizations and Single-Cell Performances. *Nanoscale Res Lett*; 2018. p. 1–13.
- [9] Md Ishak NAI, Kamarudin SK, Timmiati SN. Green synthesis of metal and metal oxide nanoparticles via plant extracts: an overview. *Mater Res Express* 2019;6:1–13. doi: <https://doi.org/10.1088/2053-1591/ab4458>.
- [10] Mittal AK, Chisti Y, Banerjee UC. Synthesis of metallic nanoparticles using plant extracts. *Biotechnol Adv* 2013;31:346–56. doi: <https://doi.org/10.1016/j.biotechadv.2013.01.003>.
- [11] Sreeju N, Rufus A, Philip D. Microwave-assisted rapid synthesis of copper nanoparticles with exceptional stability and their multifaceted applications. *J Mol Liq* 2016;221:1008–21. doi: <https://doi.org/10.1016/j.molliq.2016.06.080>.
- [12] Sangaonkar GM, Pawar KD. *Garcinia indica* mediated biogenic synthesis of silver nanoparticles with antibacterial and antioxidant activities. *Colloids Surfaces B Biointerfaces* 2018;164:210–7. doi: <https://doi.org/10.1016/j.colsurfb.2018.01.044>.
- [13] Song JY, Kwon EY, Kim BS. Biological synthesis of platinum nanoparticles using *Diopyros kaki* leaf extract. *Bioprocess Biosyst Eng* 2010;33:159–64. doi: <https://doi.org/10.1007/s00449-009-0373-2>.
- [14] Zheng B, Kong T, Jing X, Odoom-Wubah T, Li X, Sun D, et al. Plant-mediated synthesis of platinum nanoparticles and its bioreductive mechanism. *J Colloid Interface Sci* 2013;396:138–45. doi: <https://doi.org/10.1016/j.jcis.2013.01.021>.
- [15] Dauthal P, Mukhopadhyay M. Biofabrication, characterization, and possible bio-reduction mechanism of platinum nanoparticles mediated by agro-industrial waste and their catalytic activity. *J Ind Eng Chem* 2015;22:185–91. doi: <https://doi.org/10.1016/j.jiec.2014.07.009>.
- [16] Şahin B, Aygün A, Gündüz H, Şahin K, Demir E, Akocak S, et al. Cytotoxic Effects of Platinum Nanoparticles Obtained from Pomegranate Extract by the Green Synthesis Method on the MCF-7 Cell Line. *Colloids Surfaces B Biointerfaces* 2017. doi: <https://doi.org/10.1016/j.colsurfb.2017.12.042>.
- [17] Mystrioti C, Xanthopoulou TD, Tsakiridis PE, Papassiopi N, Xenidis A. Comparative evaluation of five plant extracts and juices for nanoion synthesis and application for hexavalent chromium reduction. *Sci Total Environ* 2016;539:105–13. doi: <https://doi.org/10.1016/j.scitotenv.2015.08.091>.
- [18] del Río JC, Marques G, Lino AG, Lima CF, Colodette JL, Gutiérrez A. Lipophilic phytochemicals from sugarcane bagasse and straw. *Ind Crops Prod* 2015;77:992–1000. doi: <https://doi.org/10.1016/j.indcrop.2015.09.064>.
- [19] Zhao Y, Chen M, Zhao Z, Yu S. The antibiogenic activity and mechanisms of sugarcane (*Saccharum officinarum* L.) bagasse extract against food-borne pathogens. *Food Chem* 2015;185:112–8. doi: <https://doi.org/10.1016/j.foodchem.2015.03.120>.
- [20] Arif S, Batool A, Nazir W, Khan RS, Khalid N. Physicochemical Characteristics Nutritional Properties and Health Benefits of Sugarcane Juice. *Elsevier Inc.*; 2019. doi:10.1016/B978-0-12-815270-6.00008-6.
- [21] Boligon AA, Athayde ML, Ahmad SD, Abbas SR, Sabir SM. Phenolic profile, antioxidant potential and DNA damage protecting activity of sugarcane (*Saccharum officinarum*). *Food Chem* 2013;147:10–6. doi: <https://doi.org/10.1016/j.foodchem.2013.09.113>.
- [22] Bartolomé AP, Rupérez P, Fúster C. Pineapple fruit: morphological characteristics, chemical composition and sensory analysis of red Spanish and Smooth Cayenne cultivars. *Food Chem* 1995;53:75–9. doi: [https://doi.org/10.1016/0308-8146\(95\)95790-D](https://doi.org/10.1016/0308-8146(95)95790-D).
- [23] Omorotionmwan FO, Ogwu MC. ANTIBACTERIAL CHARACTERISTICS AND BACTERIA COMPOSITION OF PINEAPPLE (*Ananas comosus* [Linn .] Merr .) PEEL AND PULP Original Article / Full Paper Introduction 2019;5:1–11. doi:10.3153/FH19001.
- [24] Suzihaque MUH, Hashib SA, Kalthum U. Effect of Inlet Temperature on Pineapple Powder and Banana Milk Powder 2015;195:2829–38. doi:10.1016/j.sbspro.2015.06.401.
- [25] Rolim WR, Pelegrino MT, de Araújo Lima B, Ferraz LS, Costa FN, Bernardes JS, et al. Green tea extract mediated biogenic synthesis of silver nanoparticles: Characterization, cytotoxicity evaluation and antibacterial activity. *Appl Surf Sci* 2019;463:66–74. doi: <https://doi.org/10.1016/j.apsusc.2018.08.203>.
- [26] Begum S, Ahmaruzzaman M. Biogenic synthesis of SnO₂/activated carbon nanocomposite and its application as photocatalyst in the degradation of naproxen. *Appl Surf Sci* 2018;449:780–9. doi: <https://doi.org/10.1016/j.apsusc.2018.02.069>.
- [27] Fang WC, Chen FR, Tsai MC, Chou HY, Wu HC, Hsieh CK. Electrochemical deposited high-crystallinity vertical platinum nanosheets onto the carbon nanotubes directly grown on carbon paper for methanol oxidation. *Surf Coatings Technol* 2017;320:584–9. doi: <https://doi.org/10.1016/j.surfcoat.2016.10.086>.
- [28] Zengin Kurt B, Durmus Z, Sevgi E. In situ reduction of graphene oxide by different plant extracts as a green catalyst for selective hydrogenation of nitroarenes. *Int J Hydrogen Energy* 2019;44:26322–37. doi: <https://doi.org/10.1016/j.ijhydene.2019.08.090>.
- [29] Ekrami-Kakhki MS, Naeimi A, Donyagard F. Pt nanoparticles supported on a novel electrospun polyvinyl alcohol-CuO-Co₃O₄/chitosan based on *Sesbania sesban* plant as an electrocatalyst for direct methanol fuel cells. *Int J Hydrogen Energy* 2019;44:1671–85. doi: <https://doi.org/10.1016/j.ijhydene.2018.11.102>.
- [30] He LL, Zheng JN, Song P, Zhong SX, Wang AJ, Chen Z, et al. Facile synthesis of platinum-gold alloyed string-bead nanochain networks with the assistance of allantoin and their enhanced electrocatalytic performance for oxygen reduction and methanol oxidation reactions. *J Power Sources* 2015;276:357–64. doi: <https://doi.org/10.1016/j.jpowsour.2014.11.119>.
- [31] Mondal S, Malik S. Easy synthesis approach of Pt-nanoparticles on polyaniline surface: an efficient electro-catalyst for methanol oxidation reaction. *J Power Sources* 2016;328:271–9. doi: <https://doi.org/10.1016/j.jpowsour.2016.08.026>.
- [32] Prabhuram J, Wang X, Hui CL, Hsing I-M. Synthesis and Characterization of Surfactant-Stabilized Pt/C Nanocatalysts for Fuel Cell Applications. *J Phys Chem B* 2003;107:11057–64. doi: <https://doi.org/10.1021/jp0357929>.
- [33] Guo JW, Zhao TS, Prabhuram J, Wong CW. Preparation and the physical/electrochemical properties of a Pt/C nanocatalyst stabilized by citric acid for polymer electrolyte fuel cells. *Electrochim Acta* 2005;50:1973–83. doi: <https://doi.org/10.1016/j.electacta.2004.09.006>.
- [34] Yahya N, Kamarudin SK, Karim NA, Masdar MS, Loh KS, Lim KL. Durability and performance of direct glycerol fuel cell with palladium-aurum / vapor grown carbon nanofiber support. *Energy Convers Manag* 2019;188:120–30. doi: <https://doi.org/10.1016/j.enconman.2019.02.087>.
- [35] Li J, Rong H, Tong X, Wang P, Chen T, Wang Z. Platinum-silver alloyed octahedral nanocrystals as electrocatalyst for methanol oxidation reaction. *J Colloid Interface Sci* 2018;513:251–7. doi: <https://doi.org/10.1016/j.jcis.2017.11.039>.
- [36] Kong X, Cao H, Li C, Chen X. One step photochemical synthesis of clean surfaced sponge-like porous platinum with high catalytic performances. *J Colloid Interface Sci* 2017;487:60–7. doi: <https://doi.org/10.1016/j.jcis.2016.10.005>.
- [37] Wang Y, Zhang L, Li F, Gu B. A novel Pt nanosponge foil with high activity for oxygen reduction reaction. *Electrochim Acta* 2013;102:1–7. doi: <https://doi.org/10.1016/j.electacta.2013.03.178>.
- [38] Shi YC, Mei LP, Wang AJ, Yuan T, Chen SS, Feng JJ. L-Glutamic acid assisted eco-friendly one-pot synthesis of sheet-assembled platinum-palladium alloy networks for methanol oxidation and oxygen reduction reactions. *J Colloid Interface Sci* 2017;504:363–70. doi: <https://doi.org/10.1016/j.jcis.2017.05.058>.
- [39] Yang Y, Cao Y, Yang L, Huang Z, Long NV. Synthesis of Pt-Pd bimetallic porous nanostructures as electrocatalysts for the methanol oxidation reaction. *Nanomaterials* 2018;8. doi: <https://doi.org/10.3390/nano8040208>.
- [40] Yang Y, Zhang R-H, Dai Z-X, Luo L-M, Zhou X-W, Du J-J. Facile aqueous-phase synthesis and electrochemical properties of novel PtPd hollow nanocatalysts. *Electrochim Acta* 2016;212:966–72. doi: <https://doi.org/10.1016/j.electacta.2016.07.085>.
- [41] Han L, Cui P, He H, Liu H, Peng Z, Yang J. A seed-mediated approach to the morphology-controlled synthesis of bimetallic copper - Platinum alloy nanoparticles with enhanced electrocatalytic performance for the methanol oxidation reaction. *J Power Sources* 2015;286:488–94. doi: <https://doi.org/10.1016/j.jpowsour.2015.04.003>.